

1 **Suppression of NSAID-induced Small Intestinal Inflammation by Orally**

2 **Administered Redox Nanoparticles**

3

4 Sha Sha^a, Long Binh Vong^a, Pennapa Chonpathompikunlert^a, Toru Yoshitomi^a,

5 Hirofumi Matsui^{b,c}, Yukio Nagasaki^{a,b,d*}

6

7 ^aDepartment of Materials Science, Graduate School of Pure and Applied Sciences,

8 University of Tsukuba, Tsukuba, Ibaraki 305-8573, Japan

9 ^bMaster's School of Medical Sciences, Graduate School of Comprehensive Human

10 Sciences, University of Tsukuba, Tsukuba, Ibaraki 305-8573, Japan

11 ^cDivision of Gastroenterology, Graduate School of Comprehensive Human Sciences,

12 University of Tsukuba, Tsukuba, Ibaraki 305-8573, Japan

13 ^dSatellite Laboratory, International Center for Materials Nanoarchitectonics

14 (WPI-MANA), National Institute for Materials Science (NIMS), University of Tsukuba,

15 Tsukuba, Ibaraki 305-8573, Japan

16

17 * Corresponding author: Department of Materials Science, Graduate School of Pure and

18 Applied Sciences, University of Tsukuba, Tennoudai 1-1-1, Tsukuba, Ibaraki 305-8573,

1 Japan. Tel/Fax: +81 29 853 5749. *E-mail address: yukio@nagalabo.jp (Y. Nagasaki)*

2

1 **Abstract**

2 Patients regularly taking non-steroidal anti-inflammatory drugs (NSAIDs) such as
3 indomethacin (IND) run the risk of small intestinal injuries. In this study, we have
4 developed an oral nanotherapeutic by using a redox nanoparticle (RNP^O), which is
5 prepared by self-assembly of an amphiphilic block copolymer that possesses nitroxide
6 radicals as side chains of hydrophobic segment via ether linkage, to reduce
7 inflammation in mice with IND-induced small intestinal injury. The localization and
8 accumulation of RNP^O in the small intestine were determined using fluorescent-labeled
9 RNP^O and electron spin resonance. After oral administration, the values of area under
10 the concentration-time curve of RNP^O in both the jejunum and ileum tissues were about
11 40 times higher than those of low-molecular-weight nitroxide radical compounds. By
12 this specific accumulation of RNP^O in small intestine, RNP^O remarkably suppressed
13 inflammatory mediators such as myeloperoxidase, superoxide anion, and
14 malondialdehyde in the small intestines of IND-treated mice. Compared to
15 low-molecular-weight nitroxide radical compounds, RNP^O also significantly increased
16 the survival rate of mice treated daily with IND. On the basis of these results, RNP^O is
17 promising as a nanotherapeutic for treatment of inflammation in the small intestine of
18 patients receiving NSAIDs.

1 **1. Introduction**

2 Non-steroidal anti-inflammatory drugs (NSAIDs) such as aspirin and
3 indomethacin (IND) are the most commonly prescribed drugs for their antipyretic,
4 analgesic, and anti-inflammatory effects. The total consumption of NSAIDs is
5 increasing in accordance with the increase in the incidence of orthopedic and
6 cardiovascular diseases [1-3]. However, it has been reported that the use of NSAIDs
7 causes severe adverse effects including ulcers, erosions, bleeding, perforation, and
8 strictures in the gastrointestinal (GI) tract such as stomach and small intestine [4-9]. The
9 absolute number of patients with serious NSAIDs-induced GI complications is
10 increasing due to the expansion of long-term NSAIDs treatment. Though the etiology
11 and pathogenesis of NSAIDs-induced inflammation are not well understood [10],
12 several studies have reported that overproduction of reactive oxygen species (ROS) and
13 an imbalance of important antioxidants exist in the intestine of patients receiving
14 repeated doses of NSAIDs, leading to oxidative damage [8, 11-14]. Self-sustaining
15 cycles of oxidant production may amplify inflammation and mucosal injury. Thus far, it
16 has been reported that antioxidant compounds and free radical scavengers heal
17 NSAIDs-induced inflammation [15, 16]. However, orally administered
18 low-molecular-weight (LMW) compounds are not sufficiently effective due to their

1 non-specific distribution to the entire body, metabolism in the GI tract, low retention in
2 the lesion area, and undesired adverse effects.

3 To address these issues, we have developed a newly designed oral
4 nanotherapeutic using redox nanoparticles (RNP^O) with ROS scavenging potential of
5 nitroxide radicals for treatment of inflammation in the GI tract. RNP^O is a
6 core-shell-type polymeric micelle with approximately 40 nm in diameter, prepared by
7 the self-assembly of methoxy-poly(ethylene
8 glycol)-*b*-poly[4-(2,2,6,6-tetramethylpiperidine-1-oxyl)oxymethylstyrene]
9 (MeO-PEG-*b*-PMOT), which is an amphiphilic block copolymer possessing nitroxide
10 radicals as side chains of hydrophobic segment via ether linkages (Figure 1a). Thus far,
11 we have found that orally administered RNP^O specifically accumulates in the colonic
12 mucosa and effectively suppresses inflammation in mice with colitis [17]. In addition,
13 we have previously confirmed that, as RNP^O is not absorbed into the bloodstream via
14 the mesentery, it does not cause the adverse effects of nitroxide radicals in the entire
15 body [17].

16 The objective of this work was to confirm the protective effect of RNP^O on
17 NSAIDs-induced small intestinal inflammation in mice. The accumulation tendency of
18 orally administered RNP^O and the suppression of ROS and inflammation in the small

1 intestine by RNP^O were investigated in detail (Figure 1b).

2

3 **2. Materials and methods**

4 *2.1. Preparation of RNP^O*

5 RNP^O was prepared by the self-assembly of an amphiphilic block copolymer
6 (MeO-PEG-*b*-PMOT) composed of the hydrophilic PEG segment and the hydrophobic
7 poly(4-methylstyrene) segment possessing nitroxide radicals as side chains via ether
8 linkages, according to our previous study [18]. Briefly, poly(ethylene
9 glycol)-*b*-poly(chloromethylstyrene) (MeO-PEG-*b*-PCMS) was synthesized by the
10 radical telomerization of chloromethylstyrene using MeO-PEG-SH (Mn = 5000; NOF
11 corporation, Tokyo, Japan) as a telogen. The chloromethyl groups were converted to
12 2,2,6,6-tetramethylpiperidinyl-1-oxyls (TEMPOs) via a Williamson ether synthesis of
13 benzyl chloride in the MeO-PEG-*b*-PCMS block copolymer with the alkoxide of
14 4-hydroxyl-2,2,6,6-tetramethylpiperidine-1-oxyl (TEMPOL). To prepare RNP^O, the
15 MeO-PEG-*b*-PMOT was dissolved in *N,N*-dimethylformamide (Wako Pure Chemicals,
16 Osaka, Japan), and transferred into a membrane tube (SpectraPor, molecular weight
17 cut-off size: 3,500 Da, Spectrum Laboratories Inc., Savannah, GA, USA) and then
18 dialyzed for 24 h against 2 L of distilled water, which was changed after 2, 4, 8, 12, and

1 20 h. After dialysis, the diameter of the obtained particles was determined using
2 dynamic light scattering measurements (Zetasizer Nanoseries ZEN3600, Malvern
3 Instruments Ltd., Worcestershire, UK).

4

5 *2.2. Animal preparation*

6 All experiments were carried out using 6-week-old male ICR mice
7 (approximately 30 g) purchased from Charles River Japan, Inc. (Yokohama, Japan).
8 Mice were maintained in the experimental animal facilities at the University of Tsukuba.

9 All experiments were performed according to the Guide for the Care and Use of
10 Laboratory Animals Resource Center of the University of Tsukuba.

11

12 *2.3. Localization of RNP^O in the small intestine*

13 The localization of RNP^O in the small intestine was determined by fluorescent
14 rhodamine-labeled RNP^O. Rhodamine-labeled RNP^O was prepared via a thiourethane
15 bond between MeO-PEG-*b*-PMOT possessing reduced TEMPO moieties and
16 rhodamine B isothiocyanate in the presence of sodium hydride. One milliliter of
17 rhodamine-labeled RNP^O (5 mg/mL) was orally administered to mice, and the mice
18 were sacrificed at 0.5, 1, 4, and 12 h after oral administration. Residues in the ileum

1 were gently removed with phosphate buffer (pH 7.4), and 7- μ m-thick sections of ileum
2 were prepared. Localization of rhodamine-labeled RNP^O was recorded using a
3 fluorescent microscope (FL-III; Leica, Tokyo, Japan).

4

5 *2.4. Biodistribution of RNP^O*

6 One milliliter of RNP^O (13.34 mg/mL) or LMW TEMPOL (2.49 mg/mL) was
7 orally administered to mice, and the mice were sacrificed at 0.25, 0.5, 1, 4, and 12 h
8 after oral administration. It should be noted that the concentrations of nitroxide radicals
9 in RNP^O and TEMPOL were equivalent, and were adjusted by measurements of
10 electron spin resonance (ESR) spectra. The jejunum, ileum, and blood were isolated
11 after operation. The jejunum and ileum tissues were gently washed with 0.9% normal
12 saline to remove any residual food. About 1 g jejunum or 0.5 g ileum tissues were
13 homogenized in 0.5 mL of phosphate buffer (pH 7.4) containing potassium ferricyanide
14 (200 mM) on ice. The ESR signal intensities in homogenized samples were analyzed
15 using an X-band ESR spectrometer (JES-TE25X; JEOL, Tokyo, Japan) at room
16 temperature under the following conditions: frequency, 9.41 GHz; power, 10.00 mW;
17 center field, 333.3; sweep width, 5 mT; sweep time, 0.5 min; modulation, 0.1 mT; time
18 constant, 0.1 s.

1 The accumulation of RNP^O in the mucosa and muscle layers of jejunum and
2 ileum was also determined by the ESR assay. To separate the mucosa and muscle of
3 both jejunum and ileum, the methods of Rang et al. [19] and Patonet et al. [20] were
4 employed. Briefly, 1 mL of RNP^O (13.34 mg/mL) or LMW TEMPOL (2.49 mg/mL)
5 was orally administered to mice, and the mice were sacrificed at 0.5 h after
6 administration. The intestinal content was gently flushed with 0.9% normal saline. Then,
7 the jejunum and ileum were longitudinally opened and the mucosa was scraped with a
8 blunt spatula.

9

10 *2.5. Experimental design using IND-induced small intestine inflammation model in mice*

11 Small intestine inflammation in mice was induced by the oral administration of
12 IND (10 mg/kg body weight [BW]; Wako Pure Chemicals), which was suspended in
13 distilled water with 1% carboxymethylcellulose (CMC; Wako Pure Chemicals) and use
14 immediately. All mice were fasted for 24 h before the experiment and divided into the
15 following 4 groups of 5 animals each.

16 Group I (Control): mice were received with distilled water 1 h before the oral
17 administration of CMC solution (1% w/v).

18 Group II (IND): mice were received with distilled water 1 h before the oral

1 administration of IND.

2 Group III (IND + TEMPOL): mice were treated with TEMPOL (18.67 mg/kg
3 BW) 1 h before the oral administration of IND.

4 Group IV (IND + RNP^O): mice were treated with RNP^O (100 mg/kg BW with
5 same amount of TEMPOL in RNP^O) 1 h before the oral administration of IND.

6 The animals were given *ad libitum* access to food and water after the
7 administration of IND. Twelve hours after the administration of IND or CMC, the
8 animals were sacrificed by cervical dislocation and the small intestine tissues were kept
9 on ice. The intestine was gently washed with 0.9% normal saline to remove any residual
10 food. The whole small intestine was separated into the duodenum, jejunum, and ileum.
11 Five-centimeter lengths of the jejunum and ileum were isolated for hematoxylin and
12 eosin (H&E) staining. The remaining tissues were used for measurements of
13 myeloperoxidase (MPO) activity, superoxide anion production, and malondialdehyde
14 (MDA) level.

15

16 2.6. H&E staining

17 Jejunum and ileum segments of mice were opened along the antimesenteric
18 border, gently rinsed to remove fecal contents, fixed on a 4% (v/v) buffered formalin

1 solution and embedded in paraffin for use in histopathological examination.
2 Seven-micrometer-thick sections were cut, deparaffinized, hydrated and stained with
3 H&E. The histology of the small intestine was evaluated using a microscope (DM
4 RXA2; Leica, Tokyo, Japan).

5

6 *2.7. Measurement of MPO activity*

7 MPO activity was measured according to the method of Bradley et al. [21].
8 Samples of intestinal tissue from treated mice were excised and homogenized in cold 50
9 mM phosphate buffer (pH 6.0) containing 0.5% (w/v) hexadecyltrimethylammonium
10 bromide. Supernatants were collected by centrifugation for 10 min at 10,000 rpm at 4°C
11 and kept at -80°C until use. The enzymatic reaction was carried out in a 96-well plate by
12 adding 190 µL of 50 mM phosphate buffer (pH 6), 5 µL of 0.5% (w/v) *o*-dianisidine
13 hydrochloride, 10 µL of the supernatant sample, and 5 µL of 20 mM H₂O₂. After
14 allowing the reaction to proceed for 30 min at room temperature, the absorbance at 460
15 nm was measured using a plate reader (Varioskan Flash; Thermo Scientific, Tokyo,
16 Japan). MPO activity was determined by comparison to a standard MPO curve (Sigma
17 Chemical Co., St. Louis, MO, USA). The protein concentration of the supernatant
18 sample was measured using a BCA kit (Thermo Scientific Pierce Protein Research

1 Products, Rockford, IL, USA). Values are expressed as MPO units/ μ g protein.

2

3 *2.8. Measurement of production of superoxide anion*

4 Superoxide anion generation was determined by the nitro blue tetrazolium (NBT)
5 assay [22]. Samples of intestinal tissue from treated mice were collected, homogenized
6 in cold 10 mM phosphate buffer (pH 7.4), and centrifuged at 10,000 rpm at 4°C for 15
7 min to obtain the supernatant. The reaction was carried out in a 96-well plate by adding
8 the supernatant sample, 10 mM boric acid-sodium hydroxide buffer, and the enzymatic
9 reaction mixture consisting of 10 mM phosphate buffer (pH 7.4) containing 0.1 mM
10 xanthine, 0.1 mM ethylene diaminetetraacetic acid, 0.1 mM NBT, and 0.1 unit xanthine
11 oxidase in a final volume of 1 mL. After 10 min at room temperature, the absorbance at
12 560 nm was measured using a plate reader. The amount of superoxide anion was
13 calculated per wet tissue weight.

14

15 *2.9. Measurement of lipid peroxidation*

16 Lipid peroxidation was evaluated by measuring the amount of MDA, following
17 the method of Ohkawa et al. [23]. Samples of intestinal tissue from treated mice were
18 collected, homogenized in cold 0.1 mM phosphate buffer (pH 7.4), and centrifuged at

1 10,000 rpm at 4°C for 15 min. An aliquot of the supernatant was added to the reaction
2 mixture containing 8% (w/v) sodium dodecyl sulfate, 20% (v/v) acetic acid, 0.8% (w/v)
3 thiobarbituric acid, and distilled water. After incubation at 95°C for 1 h, the amount of
4 MDA formed in the reaction mixture was measured using a plate reader at an
5 absorbance of 532 nm. 1,1,3,3-tetramethoxypropane was used as the standard. The
6 protein concentration of the supernatant sample was measured using the BCA kit as
7 well as the MPO assay.

8

9 *2.10. Survival rate experiment*

10 The survival rate of mice was determined by orally administering IND (10 mg/kg
11 BW) daily for 7 d. LMW TEMPOL (18.67 mg/kg BW) and RNP^O (100 mg/kg BW)
12 were also orally administered daily at 1 h before IND administration until 7 d, and the
13 number of surviving mice was counted for 7 d.

14

15 *2.12. Statistical analysis*

16 All data are expressed as mean \pm SEM. from 5 mice per group. Statistical analysis
17 using SPSS (IBM Corp., NY, USA) was performed using one-way analysis of variance,
18 followed by Tukey's post-hoc test. A *P*-value of less than 0.05 was considered

1 significant for all statistical analyses.

2

3 **3. Results and Discussion**

4 *3.1. The specific accumulation of RNP^O in small intestine*

5 The accumulation of nanoparticles in the small intestine is one of the most
6 important features for an effective nanotherapeutic against small intestinal injury. We
7 have previously confirmed that a fairly large amount of RNP^O (ca. 15% of injected dose)
8 accumulated in the colonic mucosa by oral administration. In order to confirm the effect
9 of RNP^O on NSAID-induced injury, we examined the localization of RNP^O in the small
10 intestine using fluorescent rhodamine-labeled RNP^O. When LMW rhodamine was
11 administered orally, almost no fluorescent signal was observed at 1 h (Figure 2a). On
12 the contrary, a strong fluorescent signal of RNP^O in the mucosa area of ileum was
13 observed (Figures 2b–f). In addition, the fluorescent signal was observed until 12 h after
14 oral administration of rhodamine-labeled RNP^O, indicating that the effective
15 accumulation of RNP^O in the small intestinal area continued for at least half a day.

16 To obtain quantitative information on the tendency of RNP^O to accumulate in the
17 small intestinal areas, ESR analysis was carried out in comparison with LMW
18 TEMPOL. At 0.5 h after administration of LMW TEMPOL to mice, 4.2 and 1.4% of

1 the initial dose was observed in the jejunum and ileum areas, respectively. At 1 h after
2 administration, however, almost no ESR signal was observed, as shown in Figures 3a
3 and b. In contrast, when RNP^O was orally administrated to mice, a considerably higher
4 accumulation of RNP^O in the small intestine was observed. The values of area under the
5 concentration-time curve (AUC), an important parameter in biopharmaceuticals and
6 pharmacokinetics, of RNP^O were 3.3 and 2.1 mg·h/mL in the jejunum and ileum areas,
7 respectively, which were significantly higher than those of LMW TEMPOL (0.09 and
8 0.05 mg·h/mL) (Table 1).

9 The morphology of RNP^O in the small intestine was determined by ESR spectra.
10 At 0.5 h after oral administration, the ESR signals of LMW TEMPOL in the ileum
11 showed a sharp triplet due to an interaction between the ¹⁴N nuclei and the unpaired
12 electron (Figure 3c). In contrast, the ESR signals of RNP^O even in the ileum were
13 consistently broad (Figure 3d), and this signal was observed until 4 h after oral
14 administration, indicating that the TEMPO radicals are still located in the solid core of
15 the polymeric micelles for a long time, even in the terminal portion of small intestine.
16 This might be one of the reasons preventing its uptake into blood via the mesentery.

17 The distribution of RNP^O in the small intestine region was further investigated in
18 detail. For this objective, the mucosa and muscle of both jejunum and ileum were

1 separated, and RNP⁰ localization was investigated by ESR measurement. As shown in
2 Table 2, at 0.5 h after oral administration, the amounts of RNP⁰ in the jejunum mucosa,
3 jejunum muscle, ileum mucosa, and ileum muscle were 30.6, 7.4, 15.3, and 4.1% of the
4 initial dose, respectively. The amounts of RNP⁰ in the mucosa layer were about 4 times
5 higher than those in the muscle layer in both jejunum and ileum. These results confirm
6 that our nanoparticle specifically accumulated in the intestinal mucosa preferentially.

7 Lamprecht et al. reported that the size determines the accumulation of polystyrene
8 nanoparticles in the intestinal mucosal layer [24]. However, in the harsh environment of
9 the GI tract, which includes gastric juices with strong acid, digestive enzymes, and bile
10 acid, these polystyrene nanoparticles do not always stably maintain their sizes. Block
11 copolymers can self-assemble to form a polymeric micelle structure with a dense PEG
12 brush on the surface [25]. The optimal structure allows RNP⁰ to easily diffuse in the
13 mucosa and inflammatory areas in GI tract. Because RNP⁰ did not disintegrate even in
14 the intestinal mucosa, its nanosize of 40 nm prevented the uptake of RNP⁰ into the
15 bloodstream [17], suggesting a lack of systemic adverse effects, such as hypertension
16 [26]. Furthermore, the covalent conjugation of nitroxide radicals to the backbone of
17 polymeric micelles is another important strategy to suppress the toxicity of nitroxide
18 radicals and deliver them to a target area *in vivo* without drug leakage. Based on these

1 reasons, RNP^O is the ideal material for accumulation in the small intestine.

2

3 3.2. *The protective effect of RNP^O on IND-induced small intestinal inflammation*

4 Since it has been confirmed that orally administered RNP^O significantly
5 accumulated in the intestinal area, the ROS scavenging efficiency of RNP^O in
6 IND-induced small intestinal inflammation was examined. We have previously
7 confirmed that non-disintegrated RNP^O has a definite ROS scavenging ability *in vitro*
8 [18]. Here, the protective effects of RNP^O on IND-induced inflammation in mice were
9 investigated. In this experiment, the encapsulation of IND into the hydrophobic core of
10 RNP^O in GI tract is ignorable, because almost IND exists outside of RNP^O in GI tract,
11 which is based on the maximum IND encapsulation capacity in the hydrophobic core of
12 RNP^O (6.7 wt%) (see Supporting information). After the treatments shown in the
13 experimental section, histological assessments were performed in both the jejunum and
14 ileum areas. As shown in Figures 4b and f, gross damage, such as focal and upper
15 villous necrosis, was observed in both the jejunum and ileum of mice treated with IND,
16 compared to those of control mice (Figures 4a and e). When LMW TEMPOL was orally
17 administered prior to IND-treated mice, the jejunum area was almost similar to that of
18 control mice (Figure 4c); however, a part of a necrotic villus was observed in the ileum

1 (see arrow in Figure 4g). Since LMW TEMPOL is absorbed from the upper GI tract,
2 most of it might not reach to the ileum area. On the contrary, the histology of the small
3 intestine from RNP^O-treated mice showed almost no damage and was similar to that
4 from control mice in both the jejunum and ileum areas (Figures 4d and h).

5 The different efficiencies of pretreatment with TEMPOL and RNP^O on
6 IND-treated mice were further investigated by measuring the levels of inflammatory
7 mediators, such as MPO, superoxide anion, and MDA, which indicate the extent of
8 neutrophil invasion, oxidative stress, and lipid oxidation, respectively. As shown in
9 Figure 5a, MPO activity significantly increased in small intestine of IND-treated mice,
10 especially in ileum tissues, compared to those of control mice, indicating the increase in
11 neutrophil invasion especially in the ileum region. When LMW TEMPOL was orally
12 administered to IND-treated mice, the MPO level decreased effectively, both in jejunum
13 and in ileum (Figure 5a). However, it was not suppressed to the controlled level in the
14 ileum, indicating that LMW TEMPOL could not suppress neutrophil invasion
15 completely. On the contrary, the level of MPO decreased significantly and was almost
16 the same level as that of control both in jejunum and in ileum of mice pretreated with
17 RNP^O, indicating that RNP^O could suppress neutrophil invasion almost completely both
18 in jejunum and in ileum regions. As shown in Figure 5b, the superoxide level increased

1 significantly by IND-treatment both in jejunum and in ileum. Since the MPO level in
2 the jejunum did not increase to the level in the ileum, the higher superoxide level in the
3 jejunum might be due to the direct toxicity of IND in addition to neutrophil invasion.
4 When LMW TEMPOL was administered to the IND-treated mice, the production of
5 superoxide anion decreased in the jejunum area but not in the ileum (Figure 5b),
6 suggesting that the most of LMW TEMPOL might not reach to the ileum area,
7 consistent with the result of H&E staining, as can be seen in Figures 4c and g. When
8 RNP^O was used, the amount of superoxide anion both in the jejunum and in ileum was
9 significantly suppressed, compared to that of IND-treated mice (Figure 5b), indicating
10 that RNP^O effectively scavenged overproduced superoxide anion in IND-treated mice.
11 We also confirmed lipid oxidation by measuring the amount of MDA. As shown in
12 Figure 5c, higher amounts of oxidative products were observed in both the jejunum and
13 ileum by IND treatment. LMW TEMPOL did not decrease the amounts of these
14 oxidative compounds well, especially in the jejunum area. On the other hand, all
15 oxidative stress markers both in jejunum and in ileum tissues of mice pretreated with
16 RNP^O were significantly decreased compared to those of mice treated with IND only.
17 Importantly, these oxidative stress markers both in jejunum and in ileum tissues of mice
18 pretreated with RNP^O also showed the statistically significant differences from those

1 pretreated with LMW TEMPOL. Taken together, these results clearly indicate that
2 pretreatment with RNP^O effectively prevented IND-induced inflammation by ROS
3 scavenging, unlike LMW TEMPOL.

4 Finally, we confirmed the consequences of pretreatment with TEMPOL and
5 RNP^O in IND-treated mice by a survival experiment. It is noted that mortality was
6 induced by daily administration of IND to mice for 7 d, and TEMPOL and RNP^O were
7 administered daily, 1 h before IND administration. As shown in Figure 6, the daily
8 administration of IND caused severe damage to the small intestines of mice, leading to a
9 significant decrease in survival rate (28.6%) after 7 d treatment. However, the
10 administration of LMW TEMPOL did not result in any improvement (14.3%),
11 indicating the low efficiency of TEMPOL in reducing the IND-induced the intestinal
12 inflammation. In contrast, the survival rate of mice treated daily with RNP^O (57.1%)
13 was remarkably increased. It is emphasized that the high accumulation and long
14 retention of RNP^O in the intestinal area are critical factors to reduce IND-induced small
15 intestinal inflammation.

16

17 **4. Conclusions**

18 This study demonstrates the protective effect of orally administered RNP^O on

1 IND-induced small intestinal inflammation in mice. Compared to LMW nitroxide
2 radical compounds, RNP^O showed remarkable accumulation and long retention in the
3 jejunum and ileum, especially in the mucosa layer, resulting in effective scavenging of
4 ROS and suppression of inflammation in the small intestines of IND-treated mice. On
5 the basis of these results, we believe that the oral administration of RNP^O, prior to the
6 oral administration of NSAIDs, might become an important approach for the treatment
7 of small intestinal injury in patients regularly taking NSAIDs.

8

9 **5. References**

- 10 [1] S.H. Goodnight, Aspirin therapy for cardiovascular disease, *Curr Opin Hematol*, 3
11 (1996) 355-360.
- 12 [2] G.A. Fitzgerald, Coxibs and cardiovascular disease, *N Engl J Med*, 351 (2004)
13 1709-1711.
- 14 [3] G. Singh, G. Triadafilopoulos, Epidemiology of NSAID induced gastrointestinal
15 complications, *J Rheumatol Suppl*, 56 (1999) 18-24.
- 16 [4] W.E. Smalley, W.A. Ray, J.R. Daugherty, M.R. Griffin, Nonsteroidal
17 anti-inflammatory drugs and the incidence of hospitalizations for peptic ulcer disease in
18 elderly persons, *Am J Epidemiol*, 141 (1995) 539-545.

- 1 [5] M.M. Wolfe, D.R. Lichtenstein, G. Singh, Gastrointestinal toxicity of nonsteroidal
2 antiinflammatory drugs, *N Engl J Med*, 340 (1999) 1888-1899.
- 3 [6] G. Thieffn, L. Beaugerie, Toxic effects of nonsteroidal antiinflammatory drugs on
4 the small bowel, colon, and rectum, *Joint Bone Spine*, 72 (2005) 286-294.
- 5 [7] M.C. Allison, A.G. Howatson, C.J. Torrance, F.D. Lee, R.I. Russell, Gastrointestinal
6 damage associated with the use of nonsteroidal antiinflammatory drugs, *New Engl J*
7 *Med*, 327 (1992) 749-754.
- 8 [8] I. Bjarnason, J. Hayllar, A.J. MacPherson, A.S. Russell, Side effects of nonsteroidal
9 anti-inflammatory drugs on the small and large intestine in humans, *Gastroenterology*,
10 104 (1993) 1832-1847.
- 11 [9] K. Higuchi, E. Umegaki, T. Watanabe, Y. Yoda, E. Morita, M. Murano, S. Tokioka,
12 T. Arakawa, Present status and strategy of NSAIDs-induced small bowel injury, *J*
13 *Gastroenterol*, 44 (2009) 879-888.
- 14 [10] D. Adebayo, I. Bjarnason, Is non-steroidal anti-inflammaory drug (NSAID)
15 enteropathy clinically more important than NSAID gastropathy?, *Postgrad Med J*, 82
16 (2006) 186-191.
- 17 [11] T. Yamada, M.B. Grisham, Role of neutrophil-derived oxidants in the pathogenesis
18 of intestinal inflammation, *Klin Wochenschr*, 69 (1991) 988-994.

- 1 [12] S. Somasundaram, G. Sigthorsson, R.J. Simpson, J. Watts, M. Jacob, I.A. Tavares,
2 S. Rafi, A. Roseth, R. Foster, A.B. Price, J.M. Wrigglesworth, I. Bjarnason, Uncoupling
3 of intestinal mitochondrial oxidative phosphorylation and inhibition of cyclooxygenase
4 are required for the development of NSAID-enteropathy in the rat, *Aliment Pharmacol*
5 *Ther*, 14 (2000) 639-650.
- 6 [13] J. Basivireddy, A. Vasudevan, M. Jacob, K.A. Balasubramanian,
7 Indomethacin-induced mitochondrial dysfunction and oxidative stress in villus
8 enterocytes, *Biochem Pharmacol*, 64 (2002) 339-349.
- 9 [14] Y. Nagano, H. Matsui, M. Muramatsu, O. Shimokawa, T. Shibahara, A. Yanaka, A.
10 Nakahara, Y. Matsuzaki, N. Tanaka, Y. Nakamura, Rebamipide significantly inhibits
11 indomethacin-induced mitochondrial damage, lipid peroxidation, and apoptosis in
12 gastric epithelial RGM-1 cells, *Dig Dis Sci*, 50 Suppl 1 (2005) S76-83.
- 13 [15] K. Ganguly, S. Swarnakar, Induction of matrix metalloproteinase-9 and -3 in
14 nonsteroidal anti-inflammatory drug-induced acute gastric ulcers in mice: regulation by
15 melatonin, *J Pineal Res*, 47 (2009) 43-55.
- 16 [16] Y. Niwa, M. Nakamura, N. Ohmiya, O. Maeda, T. Ando, A. Itoh, Y. Hirooka, H.
17 Goto, Efficacy of rebamipide for diclofenac-induced small-intestinal mucosal injuries in
18 healthy subjects: a prospective, randomized, double-blinded, placebo-controlled,

- 1 cross-over study, *J Gastroenterol*, 43 (2008) 270-276.
- 2 [17] L.B. Vong, T. Tomita, T. Yoshitomi, H. Matsui, Y. Nagasaki, An orally
3 administered redox nanoparticle that accumulates in the colonic mucosa and reduces
4 colitis in mice, *Gastroenterology*, 143 (2012) 1027-1025.e3.
- 5 [18] T. Yoshitomi, A. Hirayama, Y. Nagasaki, The ROS scavenging and renal
6 protective effects of pH-responsive nitroxide radical-containing nanoparticles,
7 *Biomaterials*, 32 (2011) 8021-8028.
- 8 [19] H.P. Rang, Stimulant actions of volatile anaesthetics on smooth muscle, *Br J*
9 *Pharmacol Chemother*, 22 (1964) 356-365.
- 10 [20] W.D. Paton, M.A. Zar, The origin of acetylcholine released from guinea-pig
11 intestine and longitudinal muscle strips, *J Physiol*, 194 (1968) 13-33.
- 12 [21] P.P. Bradley, D.A. Priebat, R.D. Christensen, G. Rothstein, Measurement of
13 cutaneous inflammation - estimation of neutrophil content with an enzyme marker, *J*
14 *Invest Dermatol*, 78 (1982) 206-209.
- 15 [22] S. Toda, M. Kumura, M. Ohnishi, Effects of phenolcarboxylic acids on superoxide
16 anion and lipid peroxidation induced by superoxide anion, *Planta Med*, 57 (1991) 8-10.
- 17 [23] M. Uchiyama, M. Mihara, Determination of Malonaldehyde Precursor in Tissues
18 by Thiobarbituric Acid Test, *Anal Biochem*, 86 (1978) 271-278.

- 1 [24] A. Lamprecht, U. Schafer, C.M. Lehr, Size-dependent bioadhesion of micro- and
2 nanoparticulate carriers to the inflamed colonic mucosa, *Pharmaceut Res*, 18 (2001)
3 788-793.
- 4 [25] H. Otsuka, Y. Nagasaki, K. Kataoka, Self-assembly of poly(ethylene glycol)-based
5 block copolymers for biomedical applications, *Curr Opin Colloid In*, 6 (2001) 3-10.
- 6 [26] W.J. Welch, M. Mendonca, J. Blau, A. Karber, K. Dennehy, K. Patel, Y.S. Lao,
7 P.A. Jose, C.S. Wilcox, Antihypertensive response to prolonged tempol in the
8 spontaneously hypertensive rat, *Kidney Int*, 68 (2005) 179-187.

9
10

11 **Figure Legends**

12 **Figure 1.** Schematic illustration of RNP^O and nanotherapeutics for the treatment of
13 NSAID-induced small intestinal inflammation in mice. (a) RNP^O is prepared by
14 self-assembly of a methoxy-poly(ethylene
15 glycol)-*b*-poly(4-[2,2,6,6-tetramethylpiperidine-1-oxyl]oxymethylstyrene)
16 (MeO-PEG-*b*-PMOT) block copolymer possessing nitroxide radicals as side chains of
17 hydrophobic segment. (b) After oral administration, RNP^O accumulates in the mucosa
18 of small intestine and scavenges ROS effectively.

1

2 **Figure 2.** Localization of RNP^O in the ileum was determined with rhodamine-labeled
3 RNP^O. Mice were sacrificed 0.5, 1, 2, 4, and 12 h after the oral administration of 1 mL
4 of rhodamine-labeled RNP^O at a dose of 5 mg/mL (n = 3 mice per group), and ileum
5 sections were cut circularly. The localization of rhodamine-labeled RNP^O in the ileum
6 was analyzed by fluorescent microscopy. Scale bars = 200 μm. Lu and Se in figure
7 indicate lumen and serosa, respectively.

8

9 **Figure 3.** (a) Accumulation of LMW TEMPOL (open circle) and RNP^O (closed circle)
10 in the jejunum. After the oral administration of LMW TEMPOL or RNP^O with
11 equivalent molar amount of nitroxide radicals (14.5 μmol), the amount of nitroxide
12 radicals was measured using electron spin resonance (ESR). Data are expressed as mean
13 ± SEM. from 5 mice per group. (b) Accumulation of LMW TEMPOL (open circle) and
14 RNP^O (closed circle) in the ileum. Data are expressed as mean ± SEM. from 5 mice per
15 group. (c) The ESR spectrum of LMW TEMPOL in the ileum homogenate at 0.5 h after
16 oral administration. (d) The ESR spectrum of RNP^O in the ileum homogenate at 0.5 h
17 after oral administration.

18

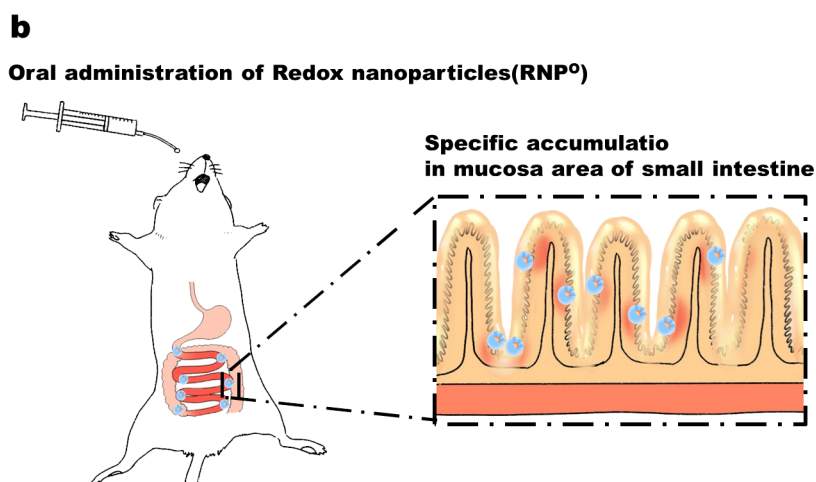
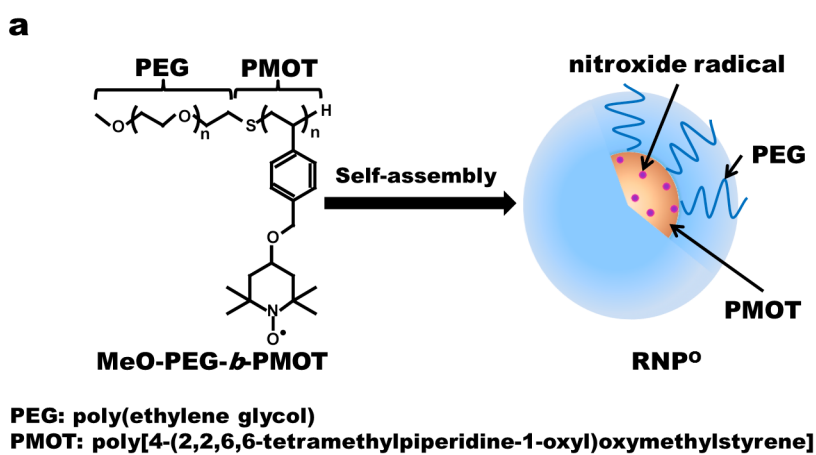
1 **Figure 4.** Histological assessments by hematoxylin and eosin (H&E) staining. At 12 h
2 after treatment, the jejunum and ileum were collected, and 7- μ m-thick sections of
3 jejunum and ileum were prepared. Sections of the jejunum and ileum were stained by
4 H&E and assessed histologically. *Red arrows* indicate the lesion areas. Scale bars = 200
5 μ m.

6
7 **Figure 5.** Protective effect of RNP^O on IND-induced small intestinal inflammation in
8 mice. At 12 h after treatment, jejunum (open bar) and ileum (closed bar) homogenates
9 were prepared, and myeloperoxidase (MPO) activity, superoxide anion generation, and
10 malondialdehyde (MDA) levels were measured. (a) MPO activity was determined by a
11 colorimetric assay using o-dianisidine hydrochloride and H₂O₂ as substrates. (b) The
12 generation of the superoxide anion was determined by the NBT assay. (c) Lipid
13 peroxidation was measured by MDA formation in intestinal tissue homogenates. Data
14 are expressed as mean \pm SEM. #*P* < 0.05 vs. control, **P* < 0.05 vs. IND, and ¶*P* < 0.05
15 vs. TEMPOL from 5 mice per group.

16
17 **Figure 6.** RNP^O increased the survival rate of mice with IND-induced small intestinal
18 inflammation. The survival rate of mice was determined following the oral

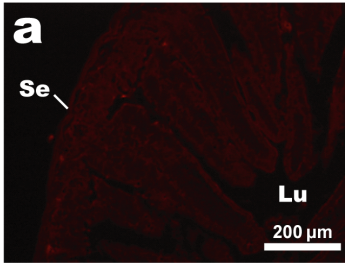
1 administration of IND (10 mg/kg BW) daily for 7 d. LMW TEMPOL (18.67 mg/kg
 2 BW) and RNP^o (100 mg/kg BW) were orally administered 1 h before IND daily for 7 d,
 3 and the number of surviving mice was counted for 7 d. n = 7 mice per group.

4

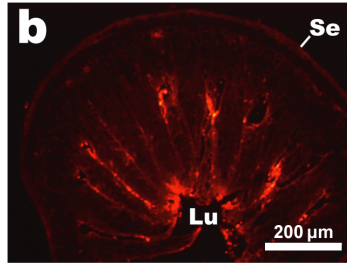


5

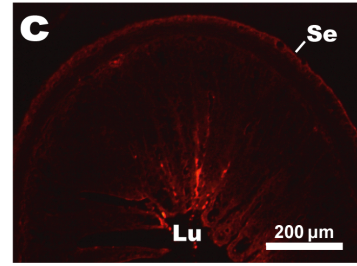
6



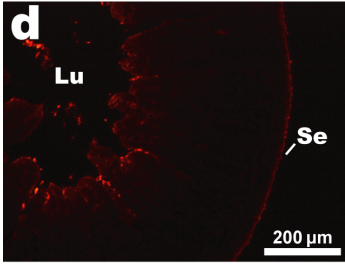
1 h Rhodamine



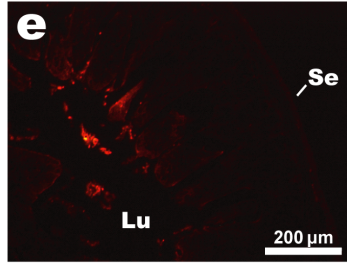
0.5h Rhodamine-RNP⁰



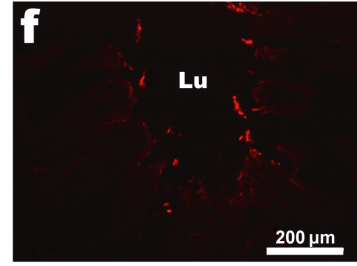
1 h Rhodamine-RNP⁰



2 h Rhodamine-RNP⁰



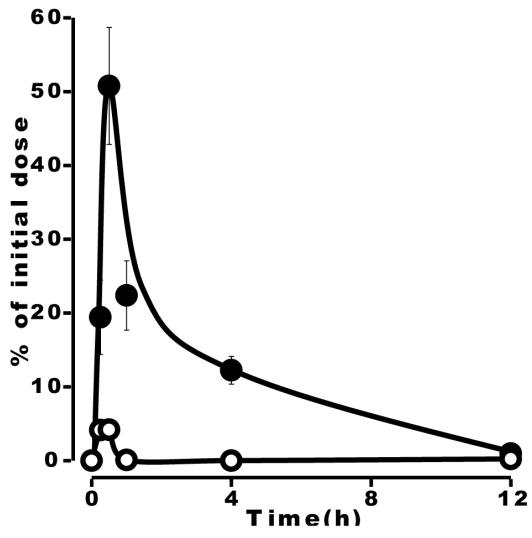
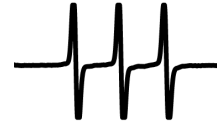
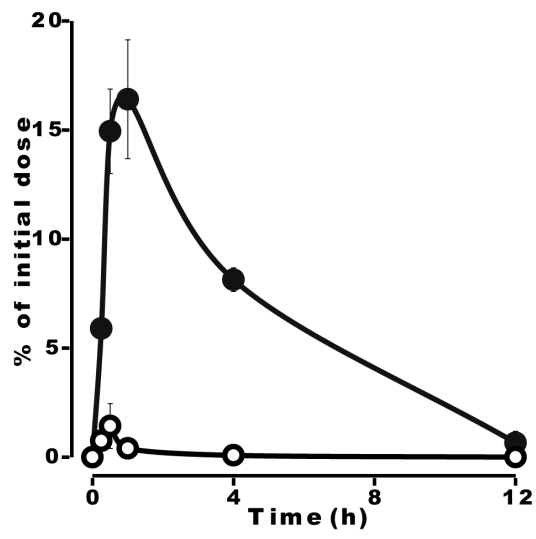
4 h Rhodamine-RNP⁰



12 h Rhodamine-RNP⁰

1

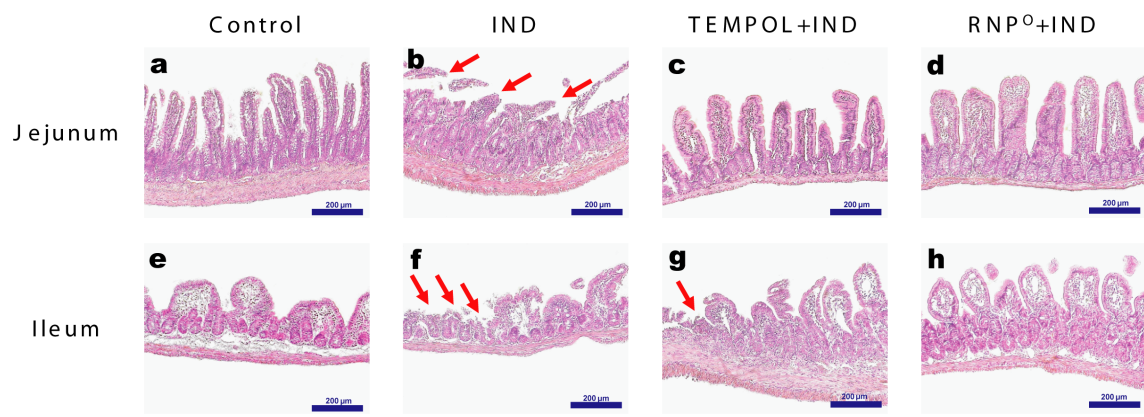
2

a**c****b****d**

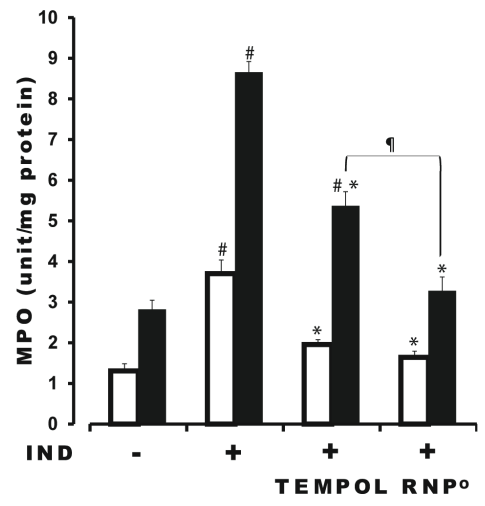
1

2

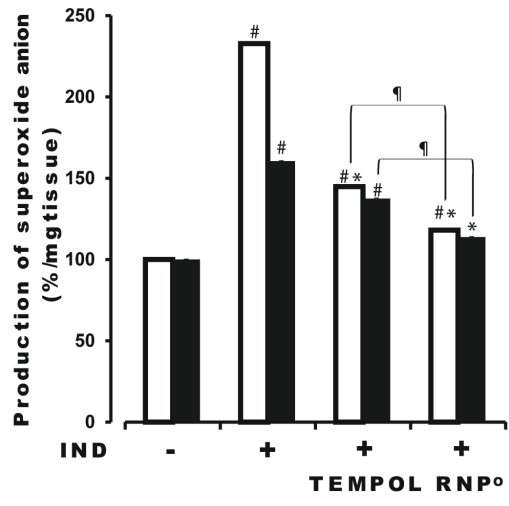
1



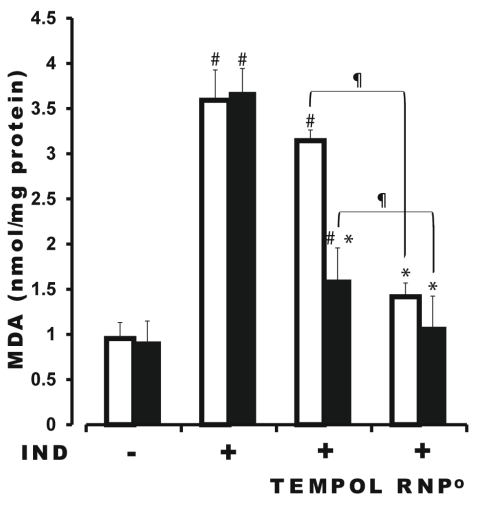
a



b

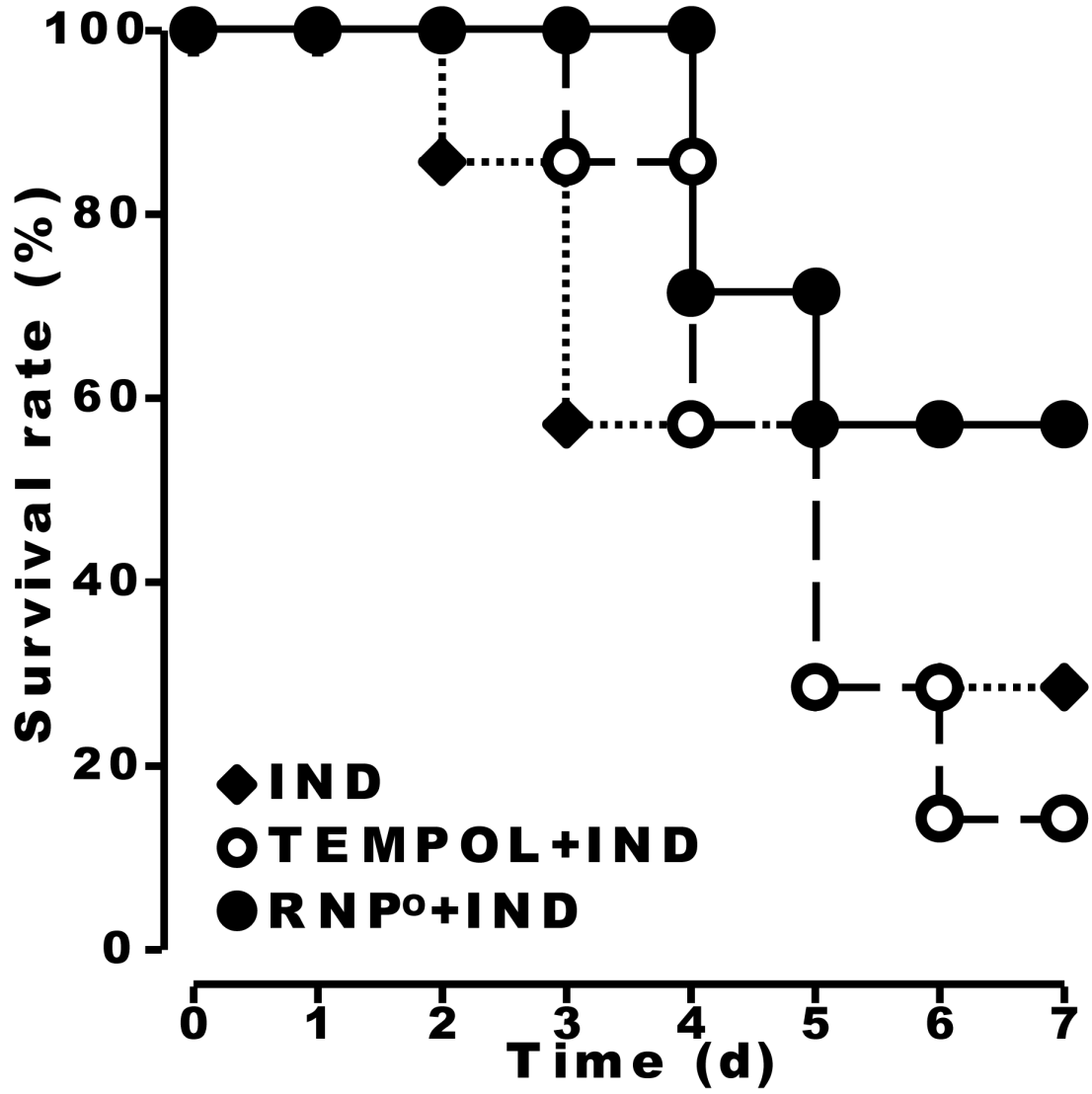


c



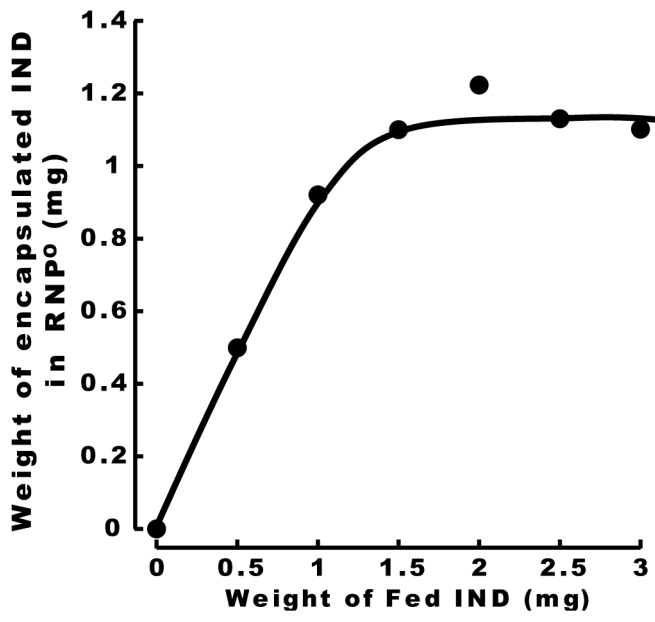
2

1



2

3



1